Thermochimica Acta 518 (2011) 72–81

Contents lists available at ScienceDirect

Thermochimica Acta

journal homepage: www.elsevier.com/locate/tca

Oxidative synthesis of a novel polyphenol having pendant Schiff base group: Synthesis, characterization, non-isothermal decomposition kinetics

Deniz Dilek[a], Fatih Doğan[a], Ali Bilici[b,*], İsmet Kaya[c]

[a] Faculty of Education, Secondary Science and Mathematics Education, Canakkale Onsekiz Mart University, 17100 Canakkale, Turkey
[b] Control Laboratory of Agricultural and Forestry Ministry, 34153 İstanbul, Turkey
[c] Department of Chemistry, Faculty of Science and Arts, Canakkale Onsekiz Mart University, Canakkale, Turkey

ARTICLE INFO

Article history:
Received 16 November 2010
Received in revised form 5 February 2011
Accepted 9 February 2011
Available online 16 February 2011

Keywords:
Oxidative polymerization
Thermal analysis
Non-isothermal decomposition kinetics

ABSTRACT

In here, the facile synthesis and thermal characterization of a novel polyphenol containing Schiff base pendant group, poly(4-{[(4-hydroxyphenyl)imino]methyl}benzene-1,2,3-triol) [PHPIMB], are reported. UV–vis, FT-IR, ^{1}H NMR, ^{13}C NMR, GPC, TG/DTG-DTA, CV (cyclic voltammetry) and solid state conductivity measurements were utilized to characterize the obtained monomer and polymer. The spectral analyses results showed that PHPIMB was composed of polyphenol main chains containing Schiff base pendant side groups. Thermal properties of the polymer were investigated by thermogravimetric analyses under a nitrogen atmosphere. Five methods were used to study the thermal decomposition of PHPIMB at different heating rate and the results obtained by using all the kinetic methods were compared with each other. The thermal decomposition of PHPIMB was found to be a simple process composed of three stages. These investigated methods were those of Flynn–Wall–Ozawa (FWO), Tang, Kissinger–Akahira–Sunose (KAS), Friedman and Kissinger methods.

1. Introduction

More recently, many studies have been reported on oxidative polymerization (OP) of phenols. OP is an alternative process for the preparation of phenolic resins without using formaldehyde [1]. This method has several advantages: no use of toxic formaldehyde, mild reaction conditions and facile procedure [2,3]. It has also been reported that the polyphenols obtained by OP consist of a mixture of phenylene and oxyphenylene units, different from the composition of conventional phenol resins [4,5]. Polymerization of various kinds of phenol monomers has been reported up till know. Some of them are phenols bearing Schiff base in their structures. OP of monohydroxy, dihydroxy phenols having Schiff base units as side group has been widely studied in acidic and alkaline medium [6–12]. Phenol monomers were also catalytically polymerized in presence of enzymes, metal complexes and metal salts [5,13,14].

monohydroxybenzene

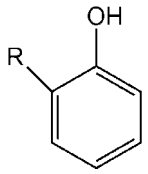

Refs. [6–10]

dihydroxybenzene

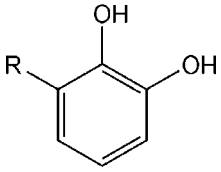

Refs. [11,12]

trihydroxybenzene

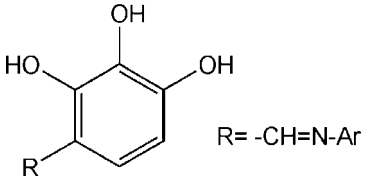

Ref. This study

However, to best of our knowledge, OP of trihydroxy substituted phenols having Schiff base units, has not been studied

* Corresponding author. Tel.: +90 212 663 39 61; fax: +90 212 663 42 96.
E-mail addresses: fatihdogan@comu.edu.tr (F. Doğan), alibilici66@hotmail.com (A. Bilici).

0040-6031/$ – see front matter © 2011 Elsevier B.V. All rights reserved.
doi:10.1016/j.tca.2011.02.009

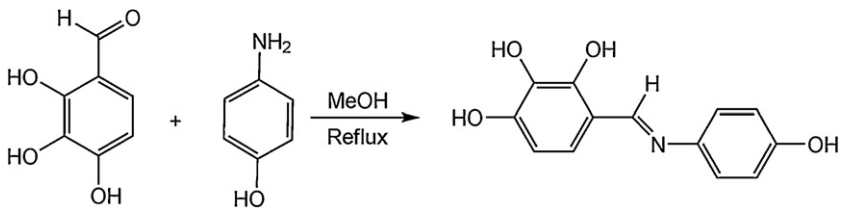

Scheme 1. The synthetic procedure for preparation of HPIMB.

in alkaline medium, up till know. In this work, the synthesis and OP of a new Schiff base, HPIMB, were studied in alkaline medium to obtain a new functional polyphenol and non-isothermal methods were used to evaluate the thermal decomposition kinetics of resulting polymer. The resulting products were also characterized by means of cyclic voltammetry, conductivity measurements.

2. Materials and methods

2.1. Materials

2,3,4-trihydroxybenzaldehyde, *p*-aminophenol and solvents were supplied from Merck Chem. Co. (Germany) and they were used as received. Sodium hypo chloride (NaOCl) (30% aqueous solution) was supplied from Paksoy Chem. Co. (Turkey).

2.2. Synthesis of 4-{[(4-hydroxyphenyl)imino]methyl}benzene-1,2,3-triol (HPIMB)

The Schiff base monomer, abbreviated as HPIMB, was synthesized by the condensation reaction of 2,3,4-trihydroxybenzaldehyde with the *p*-aminophenol. Reaction was performed as follow: *p*-aminophenol (1 mmol) was placed into a 250-mL three-necked round bottom flask which was fitted with condenser, thermometer, and magnetic stirrer, and 30 mL methanol was added into the flask as a solvent. A solution of aldehyde (1 mmol) in 20 mL methanol was added into the flask. Reaction was maintained for 3 h under reflux (Scheme 1). The precipitated Schiff base was filtered, recrystallized from methanol, and dried in vacuum desiccators.

2.3. Synthesis of poly(4-{[(4-hydroxyphenyl)imino]methyl}benzene-1,2,3-triol)

The synthesized monomer was converted to corresponding polymer derivative in an aqueous alkaline medium as described in elsewhere [10]. A solution of NaOCl (30%, in water) was used as oxidant. The synthetic pathway is given in Scheme 2.

2.4. Characterization techniques

The solubility tests of monomer and polymer were carried out by using sample of 1 mg and solvent of 1 mL at 25 °C. Electronic absorption spectra were measured using a Perkin–Elmer Lambda 25 spectrometer. The infrared spectra were obtained on Perkin Elmer Spectrum One FT-IR system using universal ATR sampling accessory within the wavelengths of 4000–550 cm^{-1}. ^{1}H NMR and ^{13}C NMR spectra (Bruker Avance DPX-400 and 100.6 MHz, respectively) were recorded at room temperature in deuterated DMSO. TMS was used as internal standard. SEC analyses were performed at 30 °C using DMF/MeOH (v/v, 4/1) as eluent at a flow rate of 0.4 mL/min. The instrument (Shimadzu 10AVp series HPLC–SEC system) was calibrated with a mixture of polystyrene standards (Polymer Laboratories; the peak molecular weights, Mp, between 162 and 19,880) using GPC software for the determination of the molecular weight (M_n), weight–average molecular weight (M_w) and polydispersity index (PDI) of the polymer sample. Macherey–Nagel GmbH & Co. (100 Å and 7.7 nm diameter loading material) 3.3 mm i.d. × 300 mm columns were used for SEC analyses. Conductivity measurements were performed on a Keithley 2400 electrometer. Samples were pressed on a hydraulic press developing to 1700 kg/cm^2. Iodine doping was carried out by exposure of the pellets to iodine vapor at atmospheric pressure in a desiccator. Electrochemical properties of monomer and polymer were determined by using a CH instrument 660B Electrochemical Analyzer in 0.1 mol L^{-1} tetrabutylamonium

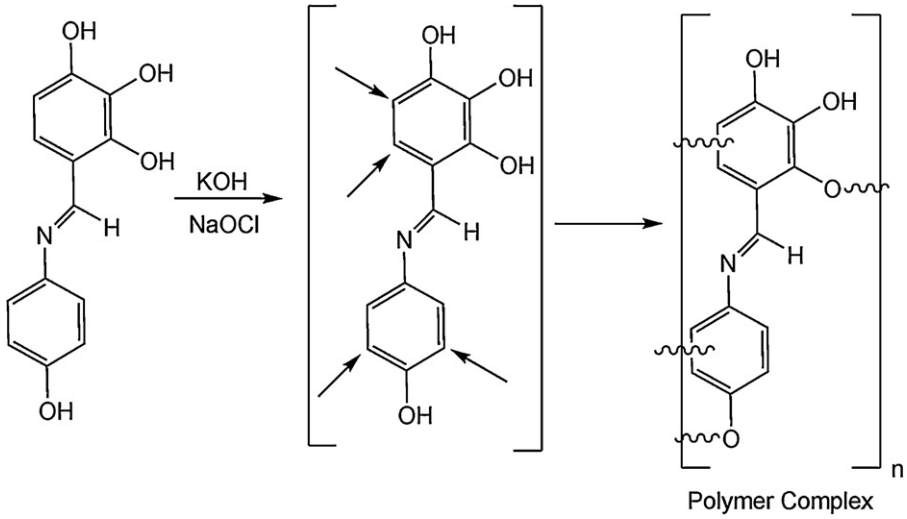

Scheme 2. The synthetic procedure for preparation of PHPIMB.

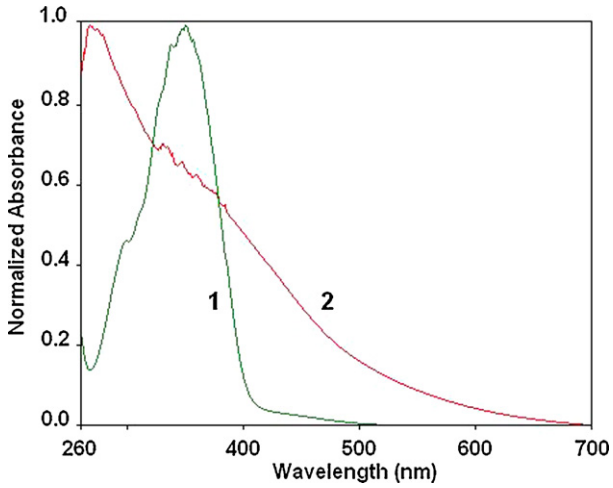

Fig. 1. UV spectra of HPIMB (1) and PHPIMB (2).

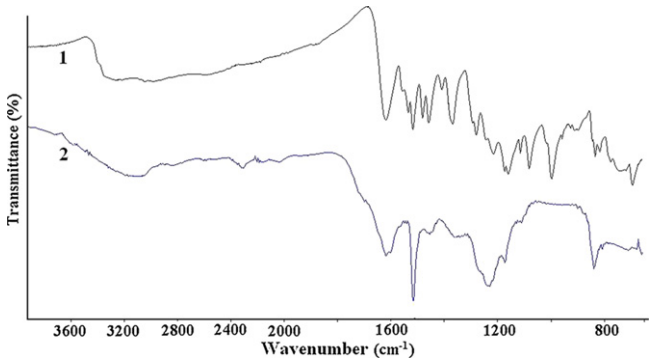

Fig. 2. FT-IR spectra of HPIMB (1) and PHPIMB (2).

hexafluorophosphate as supporting electrolyte at a potential scan rate of 20 mV s^{-1}. The voltametric measurements were performed in acetonitrile and dimethylsulfoxide under argon gas atmosphere at room temperature. The highest occupied molecular orbital (HOMO) and lowest unoccupied molecular orbital (LUMO) energy levels were calculated from oxidation and reduction onset values [15]. The TG/DTG-DTA measurements were performed using a Perkin Elmer Diamond Thermal Analysis in dynamic nitrogen atmosphere at a flow rate of 60 mL/min up to 1273 K. The heating rates were 5, 10, 15 and 20 °C/min and sample sizes ranged in mass from 8 to 10 mg. A platinum crucible was used as sample container.

3. Results and discussion

3.1. Structure of PHPIMB

PHPIMB was synthesized in two steps. The first step is based on the synthesis of Schiff base monomer via condensation reaction of protocataculaldehyde with *p*-amino phenol. In the second step, monomer synthesized is oxidized to obtain its corresponding polymer in presence of NaOCl (oxidant). The synthetic procedure for preparation of monomer and polymer are given in Schemes 1 and 2.

The polymerization of HPIMB in aqueous alkaline medium was easy to perform and the yield was quite high (95%). When the reaction temperature was 30 °C, the initial solution was pale yellow colored. However, a brownish color was developed as soon as NaOCl was added to reaction medium. During the course of the reaction, the color of solution changed from yellow to black. Polymerization reaction afforded fine and almost uniform blackish particles. The product with black colored is probably due to hydroxylation reaction developing during polymerization [16,17]. According to the SEC analysis, M_n, M_w and PDI values of PHPIMB were found to be 2980, 6280 g/mol and 2.11. These data are given as the average values of two replicates. The relatively low molecular weight of PHPIMB is consistent with its higher solubility. This polymer exhibited higher solubility in organic solvents than that of the other phenol polymers reported. [18]. PHPIMB was well soluble in common organic solvents such as DMSO, THF, DMF. However, it was partly soluble in MeOH, EtOH, chloroform, dichloromethane, ethyl acetate and insoluble in aprotic organic solvents including benzene, toluene, xylene.

The spectral characterization of resulting polymers was performed by means of UV–vis, FT-IR and NMR analyses. The UV–vis spectra of HPIMB and PHPIMB are given in Fig. 1. λ_{max} value of HPIMB was observed at 375 nm. The UV–vis spectrum of PHPIMB exhibited a blue shifted absorption maximum with a tail from 300 to 700 nm. The presence of a large absorption band from 300 to 700 nm, indicates the coexistence of both long and short effective conjugation in the polymer chains [19,20]. Optical band gap values of the synthesized compounds were also calculated as in the literature using the following equation:

$$E_g = \frac{1242}{\lambda_{on}}$$

where λ_{on} is the onset wavelength which can be determined using the absorption edges by intersection of two tangents [21]. The optical band gaps obtained for HPIMB and PHPIMB were found to be 2.79 and 2.14 eV, respectively. PHPIMB had lower band gap than its monomer compound, as expected, most probably due to its higher conjugation length.

As well known, phenol polymers consist of a mixture of phenylene and oxyphenylene units as shown in Scheme 2. HPIMB has four hydroxy groups. Therefore, it contains many coupling sites for polymerization as shown in Scheme 2. However, IR and NMR studies gave some important clues for determining the structure of PHPIMB.

FT-IR spectra of both monomer and polymer are shown in Fig. 2. PHPIMB presents bands at 3430 cm^{-1} (OH of phenolic group), 1219 and 1170 cm^{-1} (asymmetric vibrations of the C–O–C and C–OH linkages, respectively), and a peak at 1101 cm^{-1} due to the ether bond [22]. The appearance of these peaks suggests the resulting polymer is composed of a mixture of phenylene and oxyphenylene units [17].

^{1}H NMR peak assignments of HPIMB are shown in Fig. 3. The phenolic, azomethine and aromatic proton signals were appeared centered at 9.4, 8.8 and 7.3–6.4 ppm, respectively.

^{13}C NMR peak assignments of HPIMB are also given in Fig. 4. FT-IR and NMR analyses confirm the proposed monomer structure.

Fig. 5 belongs to ^{1}H NMR spectrum of a characteristic a phenol polymer. The broad signals observed between from 6.1 to 8.4 ppm are attributed to phenylene protons with the different chemical surroundings. To determine the coupling sites, the ^{1}H NMR spectrum of monomer should take part into account. It is clearly seen that the proton intensities appeared at 6.4 ppm (H_a) for monomer were drastically reduced suggesting a substantial H_a elimination during polymerization reaction. Similarly, lower proton intensities of H_b also indicate H_b elimination during polymerization. However, high H_c and H_d proton intensities show that the polymerization should take place via mainly ring A. Ring A has three hydroxyl groups and it has higher electron density of than that of ring B. Therefore, it is expected that polymerization should take place on Ring A. The phenylene/oxyphenylene contents were calculated from integration ratios of aromatic protons to hydroxyl protons and found to be 34:66.

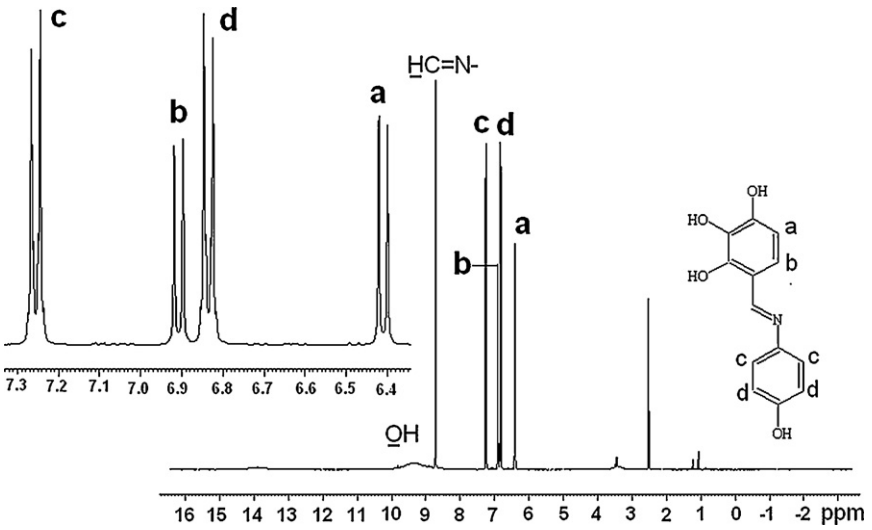

Fig. 3. ^{1}H NMR spectrum of HPIMB.

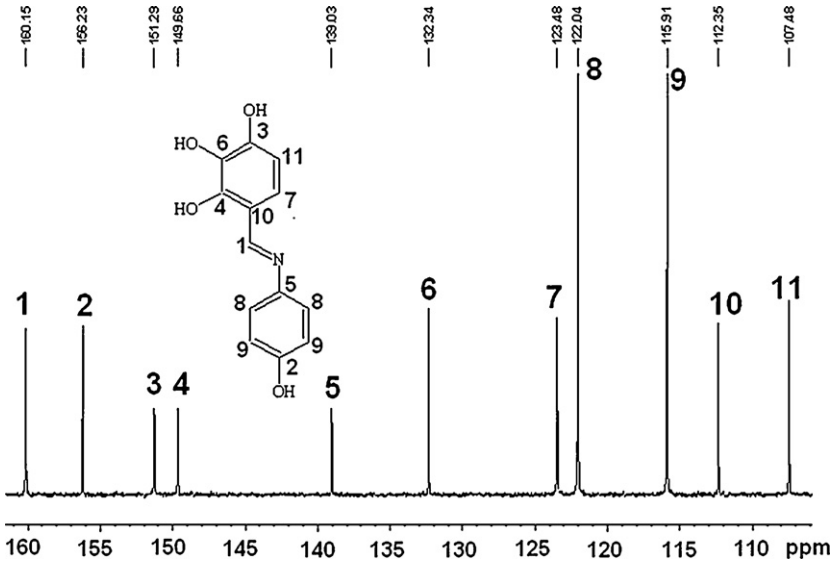

Fig. 4. ^{13}C NMR spectrum of HPIMB.

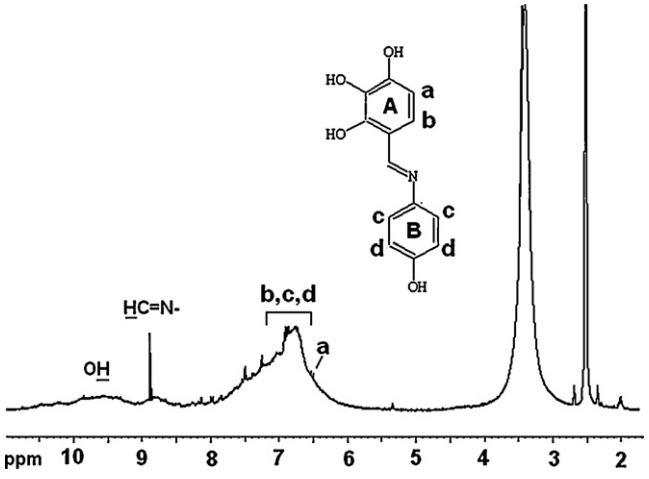

Fig. 5. ^{1}H NMR spectrum of PHPIMB.

3.2. Electrochemical properties of HPIMB and PHPIMB

CV analysis of the HPIMB and PHPIMB were carried out in acetonitrile and dimethylsulfoxide, respectively and the voltammograms are shown in Fig. 6. The HOMO, LUMO and electrochemical energy gaps (E_g') were calculated from oxidation and reduction onset values. HOMO–LUMO energy levels and electrochemical band gaps (E_g') of HPIMB and PHPIMB were found to be −5.64, −3.04; 2.60, −5.40; −3.29 and 2.11 eV, respectively. The electrochemical band gaps clearly showed that the PHPIMB synthesized by oxidative polymerization reaction had lower band gap than HPIMB due to its conjugated structure.

3.3. Electrical characteristics of HPIMB and PHPIMB

The conductivity measurements of synthesized compounds were performed on a Keithley 2400 electrometer using four-point probe technique. The pressed monomer and polymer samples (up to 1700 kg/cm^2) were exposed to iodine vapours in a desiccator up to 7 days. The results are plotted in Fig. 7. HPIMB and PHPIMB had virgin conductivities of around 10^{-11}–10^{-10} S/cm. With expo-

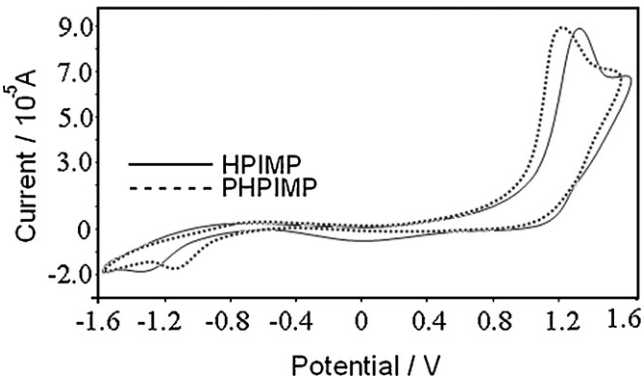

Fig. 6. Cyclic voltammograms of HPIMB and PHPIMB in solution of 0.1 M Bu_4NPF_6 at a scanning rate of 100 mV s^{-1}.

sure to iodine vapour, the conductivities of HPIMB and PHPIMB first increased significantly and then reached a plateau, suggesting the interchain and intrachain electrostatic interactions between iodine molecules and main-chain nitrogen atoms reached a saturated level. Therefore, after 72 h, the conductivity values substantially stay unchanged, even after treatment with iodine vapours (Fig. 7) The maximal (or saturated) conductivities for HPIMB and PHPIMB were found to be about 4.63×10^{-8} and 7.12×10^{-7} S/cm, respectively. From the so-called results, it was show that both HPIMB and PHPIMB had relatively higher initial and maximal conductivities than those of previously synthesized phenol polymers [23,24]. This can be result from many factor such as molecular weight, the phenylene/oxyphenylene content of resulting polymer, isolation, purification techniques ext. [25]. There are several suggested conductivity mechanisms for aromatic polymers in the literature. According to Diaz et al., nitrogen is a very electronegative element and it is capable of coordinating an iodine molecule [26]. According to Sinigersky et al. [27], the benzene rings can also be doping with iodine. A possible doping mechanism with iodine vapour for PHPIMB should be as given in Scheme 3.

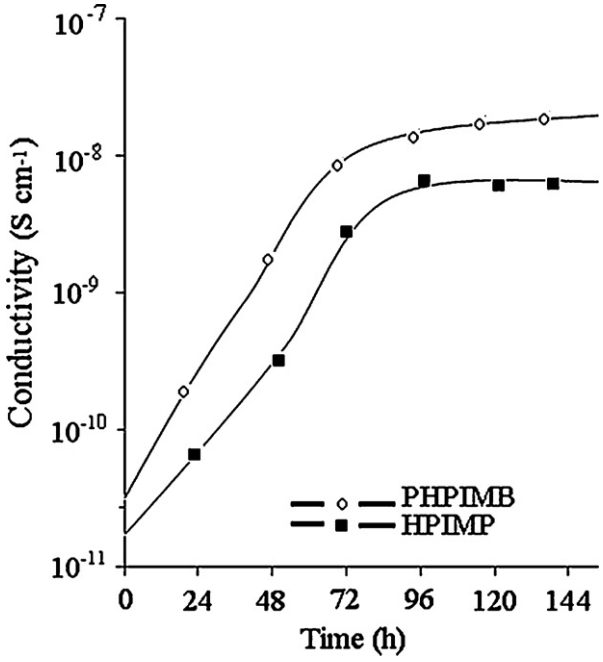

Fig. 7. Electrical conductivity of I_2-doped PHPIMB versus doping time at 25 °C.

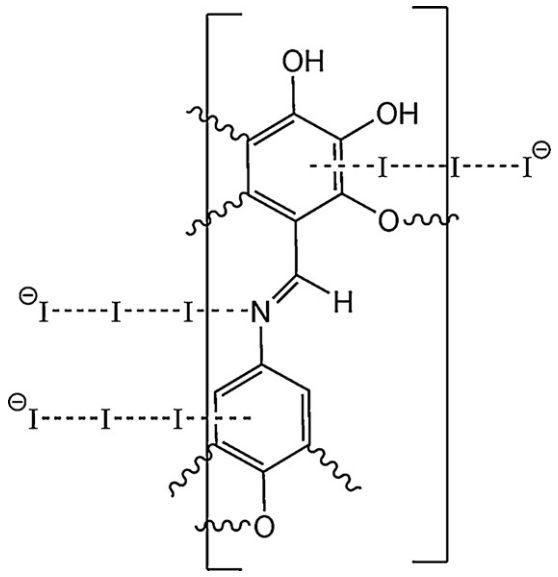

Scheme 3. Coordination of iodine during PHPIMB doping.

3.4. Thermal decomposition process

The kinetic parameters (activation energy, *E*, frequency factor, *A*) related to the thermal decomposition of PHPIMB group were determined by using multiple heating rate kinetics such as Flynn–Wall–Ozawa [28,29], Tang [30], Kissinger–Akahira–Sunose [31,32], Friedman [33] and Kissinger [31] methods. The typical dynamic TG/DTG-DTA curves of PHPIMB in a dynamic nitrogen atmosphere are given in Figs. 8–10, where the TG curves for the decomposition of 8–10 mg of PHPIMB are shown at heating rates of 5, 10, 15 and 20 °C/min under 60 mL/min nitrogen atmosphere. The solid state degradation mechanism of PHPIMB was also investigated by master plots from TG/DTG curves in N_2. The thermal decompositions of PHPIMB were very similar in character. All TG/DTG-DTA curves of PHPIMB showed that the thermal decomposition took place mainly in three stages and it is understood from TG/DTG curves, the first, second and third decomposition temperatures for PHPIMB are in range of 110–300 °C, 300–580 °C and 580–980 °C, respectively. An endothermic peak observed at about 635 °C in the DTA curve may be attributed to melting point of polymer.

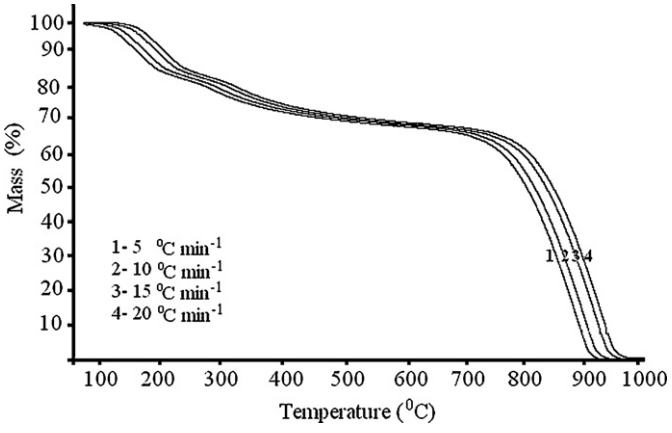

Fig. 8. TG curves of PHPIMB.

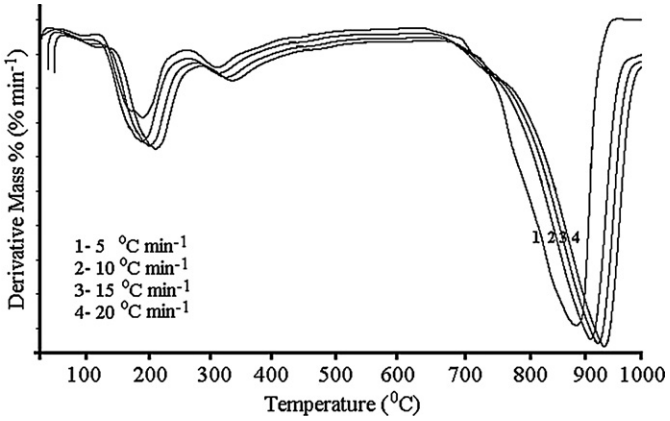

Fig. 9. DTG curves of PHPIMB.

3.4.1. Determination of kinetic triplet (activation energy E, kinetic model g(α), and pre-exponential factor, A)

First the thermogravimetric method employed to analyze the TG data of PHPIMB in this work was that of Kissinger, which is independent of heating rate and any thermal decomposition mechanisms. Kissinger method for calculating the activation energy uses the maximum decomposition temperature (T_{max}) at which the rate of mass loss is the highest. The activation energy related to thermal decomposition of PHPIMB can be calculated from the plot of ln ($\beta/T^{1.894661}$) versus 1000/T and fitting to a straight line. The mean activation energies related to the thermal decomposition of first, second and third stages of PHPIMB by using Kissinger method in N_2 was found to be 127 ± 8.43, 227 ± 8.46, and 424 ± 8.91 kJ/mol, respectively. The other methods used for calculating kinetic parameter of PHPIMB investigated are those of Flynn–Wall–Ozawa, Kissinger–Akahira–Sunose, Tang and Friedman based on multiple heating rates.

The conventional integral procedures such as FWO, KAS and Tang were proposed by assuming invariant activation energies and in the case of variable activation energies they might yield incorrect values [34]. In those cases, advanced integral isoconversional [35] or differential methods are preferred over integral isoconversional methods. Thus, in the present case, differential isoconversional methods (Friedman and Kissenger) in addition to integral isoconversional methods (FWO, KAS and Tang) were used for solid state decomposition kinetic studies.

The Flynn–Wall–Ozawa method is an integral method and the so-called Eq. (1) in logarithmic form for determining the activation energy of a solid state decomposition process without any assumption about the reaction order was suggested by Kissinger. The technique assumes that the A, $f(\alpha)$ and E are independent of T while A and E are independent of α

$$log \quad \beta = \log \frac{AE}{R} - \log \quad g(\alpha) - 2.315 - 0.4567 \quad \frac{E}{RT} \tag{1}$$

The dependence of ln (β/T^2) on 1/T, calculated for the given α values at the different heating rates β can be used to calculate the activation energy. The activation energy and the logarithmic values of the pre-exponential factor of each other thermal decomposition stage of PHPIMB calculated from FWO method were 110 ± 2.99, 29 ± 1.37; 228 ± 5.11, 31 ± 2.75; and 408 ± 7.05 kJ/mol, $49 \pm 3.57\ s^{-1}$, respectively, over the range of $0.1 < \alpha < 0.8$. On the other hand, Tang and KAS methods are an integral isoconversional method similar to the FWO. The apparent activation energy of PHPIMB can also be obtained from a plot of log β against 1000/T for a fixed degree of conversion and the slope of such a line is given by $-0.456\,E/RT$ (Eq. (2)). However, Eq. (3) suggested by KAS has also been utilized to determine the values of activation energy from plots of ln(β/T^2) against 1000/T over a wide range of conversation. Mathematical expressions of Tang and KAS methods can be written as below, respectively:

$$\ln\left(\frac{\beta}{T^{1.894661}}\right) = \ln\left(\frac{AE}{Rg(\alpha)}\right) + 3.635041 - 1.894661 \quad \ln \quad E\frac{1.001450E}{RT} \tag{2}$$

$$\ln\left[\frac{\beta}{T^2}\right] = \ln\left[\frac{AR}{Eg(\alpha)}\right] - \frac{E}{RT} \tag{3}$$

The activation energy, E, can separately be determined by a slope of logarithms plot of the left-hand side of kinetic equations versus temperature, 1/T, for a given $g(\alpha)$.

The activation energy and the logarithmic values of pre-exponential factor of PHPIMB obtained by the Tang and KAS method were found to be 110 ± 3.06, 26 ± 1.54; 109 ± 3.16, 28 ± 0.93 for the first stage, 227 ± 2.92, 30 ± 3.00; 230 ± 3.99, 32 ± 2.83 for the second stage, and 412 ± 8.46 kJ/mol, $51 \pm 3.07\ s^{-1}$; 410 ± 5.64 kJ/mol, $50 \pm 2.98\ s^{-1}$ for the third stage, respectively, over the range of $0.1 < \alpha < 0.8$.

This result agrees well with the mean values of activation energy obtained by Kissinger and FWO methods. Latest kinetic method employed in determining the activation energy of solid state thermal decomposition of PHPIMB was that of Friedman. This method used for thermal decomposition kinetic studies can be simplified as

$$\ln\left(\frac{d\alpha}{dt}\right) = \ln(A) + n \quad \ln(1-n) - \frac{E}{RT} \tag{4}$$

The E value can be calculated from the slope of a plot of ln($d\alpha/dt$) versus 1/T. The average values of activation energy and pre-exponential factor obtained for the each other stage of thermal decomposition of PHPIMB by using Friedman method were determined to be 111 ± 2.23, 28 ± 1.07; 231 ± 6.78, 31 ± 3.55; 411 ± 6.16 kJ/mol, $53 \pm 5.07\ s^{-1}$, respectively, over the range of $0.1 < \alpha < 0.8$. In the equations above α, $g(\alpha)$, β, T_m, E, A, R are the degree of reaction, integral function of conversion, heating rate, DTG peak temperature, activation energy (kJ/mol), pre-exponential factor (s^{-1}) and gas constant (8.314 J/mol K^{-1}), respectively. The activation energies calculated from the FWO, Tang, KAS and Friedman methods for all the thermal decomposition stage are summarized in Tables 1–3.

In consequently, the activation energies E values of PHPIMB calculated from all mathematical methods are very close to each other. Also, correlation coefficients of the Arrhenius type plots of dynamic

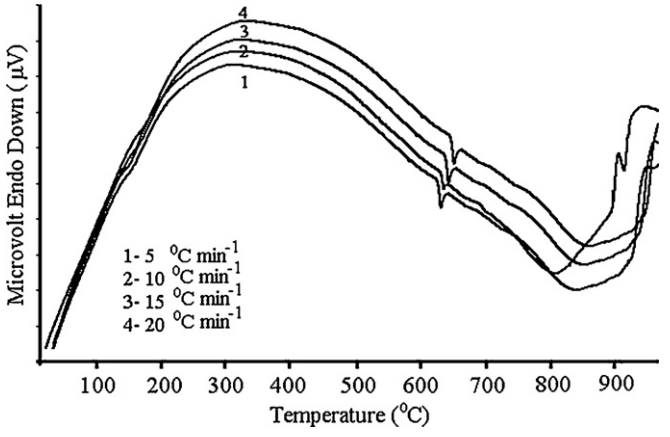

Fig. 10. DTA curves of PHPIMB.

Table 1
Activation energy values obtained by different methods for first decomposition stage.

Conversion	First thermal decomposition stage							
	Tang		KAS		FWO		Friedman	
	E	$\ln A$	E	$\ln A$	E	$\ln A$	E	$\ln A$
0.05	71 ± 6.11	20.16	70 ± 6.45	20.60	72 ± 2.75	20.00	79 ± 1.25	22.49
0.1	105 ± 6.10	24.66	104 ± 6.45	26.46	107 ± 2.70	26.46	111 ± 1.25	27.50
0.2	108 ± 6.10	25.75	107 ± 6.44	27.57	107 ± 2.65	27.08	109 ± 1.23	27.23
0.3	108 ± 6.09	25.21	108 ± 6.44	28.02	109 ± 2.62	29.28	110 ± 1.24	28.72
0.4	110 ± 6.09	27.75	110 ± 6.44	28.58	111 ± 2.60	29.63	112 ± 1.22	29.92
0.5	114 ± 6.09	28.20	113 ± 6.43	28.96	114 ± 2.57	29.94	116 ± 1.23	30.18
0.6	110 ± 6.08	27.08	109 ± 6.43	26.90	111 ± 2.55	29.72	112 ± 1.20	28.36
0.7	113 ± 6.08	28.64	113 ± 6.43	28.49	114 ± 2.52	29.65	114 ± 1.21	29.72
0.8	113 ± 6.08	28.10	112 ± 6.44	28.94	114 ± 2.45	29.94	111 ± 1.23	28.86
0.9	152 ± 6.09	32.95	152 ± 6.44	32.04	153 ± 2.41	32.32	154 ± 1.22	34.22
0.95	210 ± 6.09	39.03	209 ± 6.46	39.41	207 ± 2.39	38.81	214 ± 1.24	39.11
$0.05 < \alpha < 0.95$	119 ± 35.16	27 ± 5.07	118 ± 35.18	29 ± 3.78	124 ± 31.91	29 ± 4.47	126 ± 33.59	29 ± 4.19
$0.1 < \alpha < 0.8$	110 ± 3.06	26 ± 1.54	109 ± 3.16	28 ± 0.93	110 ± 2.99	28 ± 1.37	111 ± 2.23	28 ± 1.07

Table 2
Activation energy values obtained for second decomposition stage.

Conversion	Second thermal decomposition stage							
	Tang		KAS		FWO		Friedman	
	E	$\ln A$	E	$\ln A$	E	$\ln A$	E	$\ln A$
0.05	157 ± 5.32	27.24	156 ± 5.41	28.34	158 ± 2.11	28.54	169 ± 1.48	29.23
0.1	244 ± 5.31	38.56	249 ± 5.40	40.36	248 ± 2.09	39.54	251 ± 1.48	40.56
0.2	230 ± 5.30	35.08	231 ± 5.39	35.84	231 ± 2.10	35.58	239 ± 1.48	37.76
0.3	224 ± 5.32	28.40	226 ± 5.40	30.93	224 ± 2.09	29.56	230 ± 1.47	30.82
0.4	229 ± 5.31	33.50	229 ± 5.38	33.27	234 ± 2.08	33.61	236 ± 1.47	34.33
0.5	224 ± 5.30	27.34	228 ± 5.39	29.72	219 ± 2.08	28.71	226 ± 1.48	29.51
0.6	221 ± 5.29	27.39	221 ± 5.39	27.20	220 ± 2.08	27.24	222 ± 1.46	28.80
0.7	226 ± 5.28	29.98	235 ± 5.37	33.80	227 ± 2.08	30.30	224 ± 1.46	27.34
0.8	226 ± 5.28	29.53	228 ± 5.36	29.32	226 ± 2.07	29.27	221 ± 1.45	27.74
0.9	224 ± 5.26	27.00	228 ± 5.36	29.81	228 ± 2.07	29.36	234 ± 1.47	30.09
0.95	257 ± 5.26	39.79	257 ± 5.35	40.60	256 ± 2.07	41.13	264 ± 1.51	43.41
$0.05 < \alpha < 0.95$	223 ± 24.60	31 ± 4.72	226 ± 25.30	32 ± 4.62	224 ± 24.84	32 ± 4.73	228 ± 23.72	32 ± 5.53
$0.1 < \alpha < 0.8$	227 ± 2.92	30 ± 3.00	230 ± 3.99	32 ± 2.83	228 ± 5.11	31 ± 2.75	231 ± 6.78	31 ± 3.55

TG/DTG runs for all stages in the decomposition of PHPIMB for activation energy given in Tables 1–3 are considerably higher for masses ranging from $\alpha = 0.1$ to 0.8 in N_2. It was also found that the standard deviation values of activation energies which are obtained for a range of $0.1 < \alpha < 0.8$ were smaller than those values obtained for a given α ($0.05 < \alpha < 0.95$). Thus, the activation energies related to corresponding decomposition steps of polymer were estimated in range of $0.1 < \alpha < 0.8$. These results indicate that activation energies related to the smaller and biggest values of α have big effect on the standard deviation.

Fig. 11 shows the E-dependencies degree of conversion, α in TG runs in N_2. The E-dependencies for each stage of PHPIMB in N_2 presents a similar behavior for the all the methods. The activation energy values obtained for each stages of thermal decomposition

Table 3
Activation energy values obtained for third decomposition stage.

Conversion	Third thermal decomposition stage							
	Tang		KAS		FWO		Friedman	
	E	$\ln A$	E	$\ln A$	E	$\ln A$	E	$\ln A$
0.05	346 ± 6.21	48.45	345 ± 6.59	48.20	342 ± 2.17	47.75	335 ± 2.15	48.45
0.1	404 ± 6.27	48.66	410 ± 6.66	49.60	416 ± 2.18	50.94	417 ± 2.15	51.72
0.2	404 ± 6.29	47.84	403 ± 6.68	46.74	396 ± 2.18	45.58	405 ± 2.14	47.89
0.3	410 ± 6.30	49.38	409 ± 6.70	47.27	405 ± 2.18	46.17	407 ± 2.14	47.05
0.4	404 ± 6.31	47.20	403 ± 6.71	46.08	400 ± 2.19	44.15	402 ± 2.13	46.38
0.5	416 ± 6.32	51.47	414 ± 6.71	52.38	411 ± 2.19	51.78	415 ± 2.13	58.74
0.6	417 ± 6.32	51.35	415 ± 6.72	52.19	411 ± 2.19	52.24	416 ± 2.13	58.22
0.7	422 ± 6.33	54.75	418 ± 6.73	53.64	413 ± 2.19	53.01	416 ± 2.12	58.27
0.8	425 ± 6.34	55.46	415 ± 6.74	52.28	413 ± 2.20	52.17	417 ± 2.13	58.86
0.9	482 ± 6.35	65.14	499 ± 6.75	66.22	493 ± 2.20	65.64	501 ± 2.12	62.11
0.95	531 ± 6.37	69.72	530 ± 6.77	68.84	522 ± 2.21	68.65	529 ± 2.13	66.87
$0.05 < \alpha < 0.95$	423 ± 47.33	53 ± 7.41	423 ± 49.70	53 ± 7.62	420 ± 48.26	52 ± 7.85	423 ± 51.29	54 ± 6.95
$0.1 < \alpha < 0.8$	412 ± 8.46	51 ± 3.07	410 ± 5.64	50 ± 2.98	408 ± 7.05	49 ± 3.57	411 ± 6.16	53 ± 5.07

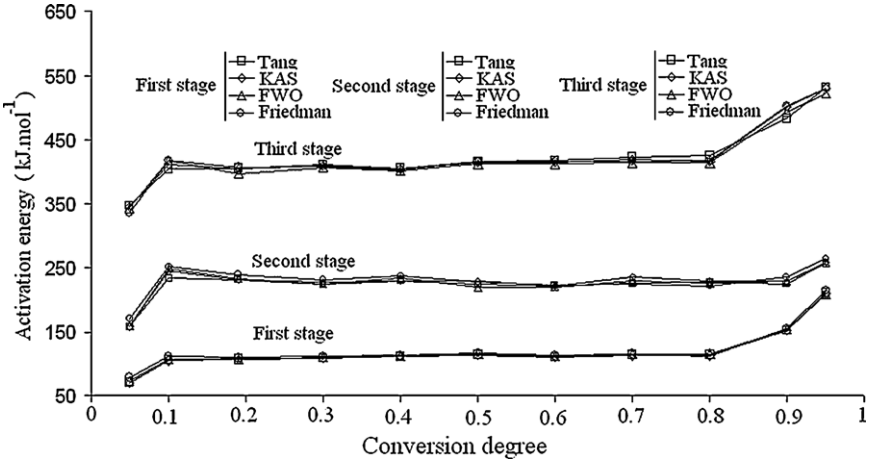

Fig. 11. The E_a-dependencies obtained for the thermal decomposition of PHPIMB studied in TG/DTG run in N_2.

of PHPIMB in conversion ranging from $\alpha = 0.1$ to 0.8 is very close. This result indicates that the mechanism of all the stages does not change in the region $0.1 < \alpha < 0.8$.

The lowest values of activation energy required for initial decomposition were found to be approximately 70 ± 6.45 and 156 ± 5.41 kJ/mol, respectively, by using KAS method for first and second decomposition stage and 335 ± 2.15 kJ/mol by using Friedman method for three ones, over the range of $0.1 < \alpha < 0.95$.

3.4.2. Determination of the kinetic model by master plots

The integral function of conversion in the solid state non-isothermal decomposition reactions is expressed as

$$g(\alpha) = \left(\frac{A}{\beta}\right) \int_{T_0}^{T} \exp\left(\frac{-E}{RT}\right) dT = \left(\frac{AE}{\beta R}\right) p(u) \quad (5)$$

where $p(u) = \int_{\infty}^{u} -(e^{-u}/u^2)du$ and $u = E/RT$.

Using a reference at point $\alpha = 0.5$ and according to Eq. (2), one gets

$$g(\alpha) = \left(\frac{AE}{\beta R}\right) p(u_{0.5}) \quad (6)$$

where $u_{0.5} = E/RT$. When Eq. (2) is divided by Eq. (6), the following equation is obtained

$$\frac{g(\alpha)}{g(0.5)} = \frac{p(\alpha)}{p(u_{0.5})} \quad (7)$$

Plots of $g(\alpha)/g(0.5)$ against α correspond to theoretical master plots of various $g(\alpha)$ functions given in Table 4. To draw the experimental master plots of $p(u)/p(u_{0.5})$ against α from experimental data obtained under different heating rates, an approximate formula [36] of $p(u)$ with high accuracy is used $p(u) = \exp(-u)/[u(1.00198882u + 1.87391198)]$. Eq. (7) indicates that, for a given α, the experimental value of $g(\alpha)/g(\alpha_{0.5})$ are equivalent when an appropriate kinetic model is used. Comparing the experimental master plots with theoretical ones can conclude the kinetic model.

In order to find out the most likely thermal decomposition mechanism of each stage of PHPIMB, we chose master plots in which plots of $g(\alpha)/g(0.5)$ against α correspond to theoretical master plots of various $g(\alpha)$ functions [37–41]. Comparing the experimental master plots with theoretical ones we can be determine the kinetic model related to the thermal decomposition of each stage of PHPIMB [42]. In order to confirm the thermal decomposition mechanisms of PHPIMB, the theoretical master plots of various kinetic functions against α constructed from experimental data obtained for thermal decomposition stages of PHPIMB under

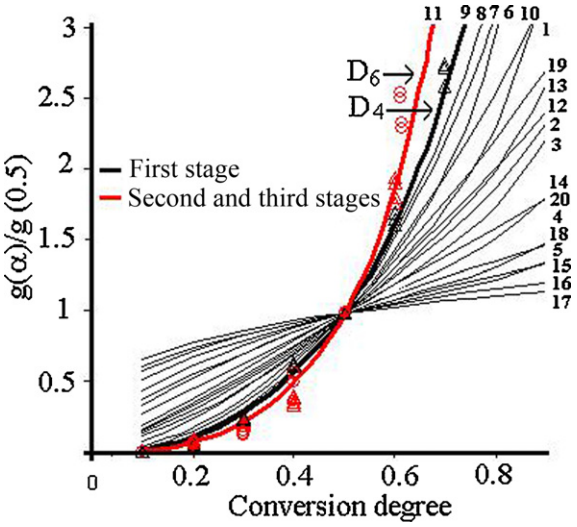

Fig. 12. Master plots of theoretical $g(\alpha)/g(0.5)$ against α for various reaction models (solid curves represent 20 kinds of reaction models given in Refs. [33–36]) and experimental data [(△), (▲) and (○)] of PHPIMB at the heating rates 5, 10, 15 and 20 °C/min.

different heating rates in N_2 was compared each other. The comparisons of the experimental and theoretical master curves show that the kinetic process of the thermal decomposition of PHPIMB agree with, the D_4 master curve for the first decomposition stage, the D_6 master curve for the second and third decomposition stage, very well (see Fig. 12). In the literature, D_4 model is also known as Ginstling–Brounshtein equation [43]. On the other hand, D_6 kinetic model is known as Komatsu–Uemura or anti-Jander equation [44]. D_4 model has a three-dimensional diffusion type decomposition mechanism while D_6 model has a three-dimensional counter-diffusion type decomposition mechanism.

Experimental data, the mathematical expressions of the D_4 and D_6 master curves, and the average reaction energy predetermined obtained for each stage of the thermal decomposition were subtracted into Eq. (5), the following equation can be deduced

$$(8)\ln\left[\frac{\beta R}{E}\right] - \ln[p(u)] = \ln \quad A - \ln\left[1 - (1-\alpha)^{1/3}\right]^2$$

For first thermal decomposition stage

$$(9)\ln\left[\frac{\beta R}{E}\right] - \ln[p(u)] = \ln \quad A - \ln\left[\left[1/(1-\alpha)\right]^{1/3} - 1\right]^2$$

For second thermal decomposition stage

Table 4
Algebraic expression for the most frequently used mechanisms of solid state process.

No	Mechanisms	Symbol	Differential form, $f(\alpha)$	Integral form, $g(\alpha)$
Sigmoidal curves				
1	N and G ($n=1$)	A_1	$(1-\alpha)$	$[-\ln(1-\alpha)]$
2	N and G ($n=1.5$)	$A_{1.5}$	$(3/2)(1-\alpha)[-\ln(1-\alpha)]^{1/3}$	$[-\ln(1-\alpha)]^{2/3}$
3	N and G ($n=2$)	A_2	$2(1-\alpha)[-\ln(1-\alpha)]^{1/2}$	$[-\ln(1-\alpha)]^{1/2}$
4	N and G ($n=3$)	A_3	$3(1-\alpha)[-\ln(1-\alpha)]^{2/3}$	$[-\ln(1-\alpha)]^{1/3}$
5	N and G ($n=4$)	A_4	$4(1-\alpha)[-\ln(1-\alpha)]^{3/4}$	$[-\ln(1-\alpha)]^{1/4}$
Deceleration curves				
6	Diffusion, 1D	D_1	$1/(2\alpha)$	α^2
7	Diffusion, 2D	D_2	$1/(\ln(1-\alpha))$	$(1-\alpha)\ln(1-\alpha)+\alpha$
8	Diffusion, 3D	D_3	$1.5/[(1-\alpha)^{-1/3}-1]$	$(1-2\alpha/3)-(1-\alpha)^{2/3}$
9	Diffusion, 3D	D_4	$[1.5(1-\alpha)^{2/3}]\,[1-(1-\alpha)^{1/3}]^{-1}$	$[1-(1-\alpha)^{1/3}]^2$
10	Diffusion, 3D	D_5	$(3/2)(1+\alpha)^{2/3}[(1+\alpha)^{1/3}-1]^{-1}$	$[(1+\alpha)^{1/3}-1]^2$
11	Diffusion, 3D	D_6	$(3/2)(1-\alpha)^{4/3}[[1/(1-\alpha)^{1/3}]-1]^{-1}$	$[[1/(1-\alpha)]^{1/3}-1]^2$
12	Contracted geometry shape (cylindrical symmetry)	R_2	$(1-\alpha)^{1/3}$	$2(1-\alpha)^{1/2}$
13	Contracted geometry shape (sphere symmetry)	R_3	$(1-\alpha)^{2/3}$	$3(1-\alpha)^{1/3}$
Acceleration curves				
14	Mample power law	P_1	1	α
15	Mample power law ($n=2$)	P_2	$2\alpha^{1/2}$	$\alpha^{1/2}$
16	Mample power law ($n=3$)	P_3	$(1.5)\alpha^{2/3}$	$\alpha^{1/3}$
17	Mample power law ($n=4$)	P_4	$4\alpha^{3/4}$	$\alpha^{1/4}$
18	Mample power law ($n=2/3$)	$P_{3/2}$	$2/3(\alpha)^{-1/2}$	$\alpha^{3/2}$
19	Mample power law ($n=3/2$)	$P_{2/3}$	$3/2(\alpha)^{1/3}$	$\alpha^{2/3}$
20	Mample power law ($n=4/3$)	$P_{3/4}$	$4/3(\alpha)^{-1/3}$	$\alpha^{3/4}$

$$(10)\ln\left[\frac{\beta R}{E}\right]-\ln[p(u)]=\ln\quad A-\ln\left[[1/(1-\alpha)]^{1/3}-1\right]^2$$

For third thermal decomposition stageThe plots of $\ln[\beta R/E]$–$\ln[p(u)]$ versus – $\ln[1-(1-\alpha)^{1/3}]^2$, $-\ln[[1/(1-\alpha)]^{1/3}-1]^2$ for second and third stages, give a group of straight lines. The pre-exponential factor can be obtained from the intercepts of the regression lines corresponding to various heating rates. By assuming the theoretical D_4 and D_6 laws, the logarithmic value of the pre-exponential factor, $\ln A$ obtained from correlation coefficient of the plots of $\ln[\beta R/E]-\ln[p(u)]$ versus – $\ln[1-(1-\alpha)^{1/3}]^2$ for first decomposition stage were found to be $29\pm0.15\,s^{-1}$. Also, $\ln A$ values by a plots of $\ln[\beta R/E]-\ln[p(u)]$ versus – $\ln[[1/(1-\alpha)]^{1/3}-1]^2$ for second and third stages were 33 ± 1.06 and $45\pm0.08\,s^{-1}$, respectively.

4. Conclusions

A new Schiff base, HPIMB, was synthesized and oxidatively polymerized in an aqueous alkaline medium in presence of NaOCl. The resulting polymer was relatively soluble in organic solvents. M_n, M_w and PDI values of PHPIMB were found to be 2980, 6280 g/mol and 2.11, respectively. The electrical conductivity of PHPIMB increased monotonically from 10^{-10} to 7.12×10^{-7} S/cm with increasing doping time from 0 to 7 days. The average values of activation energy of the thermal decomposition of PHPIMB obtained by the Tang, KAS, FWO, Friedman and Kissinger methods were found to be 110 ± 3.06, 109 ± 3.16, 110 ± 2.99, 111 ± 2.23 and 127 ± 8.43 kJ/mol for the first stage, respectively, over the range of $0.1<\alpha<0.8$. On the other hand, The average values of activation energies related to the second and third decomposition stages obtained by so-called methods for the given α values were 227 ± 2.92, 230 ± 3.99, 228 ± 5.11, 231 ± 6.78 and 227 ± 8.46, and 412 ± 8.46, 410 ± 5.64, 408 ± 7.05, 411 ± 6.16, 424 ± 8.91 kJ/mol, respectively. Analysis of the results obtained by master plots method showed that the decomposition mechanism of PHPIMB in N_2 went to D_n mechanism (Deceleration type) for both stages and pre-exponential factors related to the each other thermal decomposition stage were determined to be 29 ± 0.15, 33 ± 1.06 and $45\pm0.08\,s^{-1}$, respectively. It is noted that a diffusion type kinetic model is suggested in here. This kinetic model is quite rare in polymer degradation studies and it has been reported in the literature that thermal degradation of polyethylene follows a diffusion kinetic model [45,46].

Acknowledgement

Dr. Fatih Doğan thanks to Canakkale Onsekiz Mart University Research Fund for support with the project (COMU Project No: 2010/119)

References

[1] Y.J. Kim, H. Uyama, S. Kobayashi, Peroxidase-catalyzed oxidative polymerization of phenol with a nonionic polymer surfactant template in water, Macromol. Biosci. 4 (2004) 497–502.
[2] H. Mart, Oxidative polycondensation reaction, Des. Monomers Polym. 9 (2006) 551–588.
[3] I. Kaya, D. Emdi, M. Sacak, Synthesis, characterization and antimicrobial properties of oligomer and monomer/oligomer-metal complexes of 2-[(pyridine-3-yl-methylene)amino]phenol, J. Inorg. Organomet. Polym. 19 (3) (2009) 286–297.
[4] S.I. Tawaki, Y. Uchida, Y. Maeda, I. Ikeda, HRP-catalyzed polymerization of sugar-based phenols in aqueous organic solvents, Carbohydr. Polym. 59 (2005) 71–74.
[5] I. Yamaguchi, T. Yamamoto, Enzymatic polymerization of a ferrocenophane to give poly(oxyphenylene) with ferrocenophane pendant groups, Inorg. Chim. Acta 348 (2003) 249–253.
[6] I. Kaya, A. Çetiner, M. Saçak, Synthesis, characterization and thermal degradation oligomer and monomer/oligomer metal complex compounds of 2-methylquinolin-8-ol, J. Macromol. Sci. Pure 44 (2007) 463–468.
[7] I. Kaya, A. Erçağ, S. Çulhaoğlu, Synthesis and characterization of oligo-2-[(2-hydroxymethylphenylimino) methyl] phenol and oligo-2-[(2-hydroxymethylphenyl imino) methyl]-4-bromo-phenol, Turk. J. Chem. 31 (2007) 55–63.
[8] I. Kaya, M. Yıldırım, Synthesis, characterization, thermal stability, conductivity and band gap of a new aromatic polyether containing an azomethine as a side, J. Appl. Polym. Sci. 106 (2007) 2282–2289.
[9] I. Kaya, A. Bilici, Syntheses, structures, electric conduction, electrochemical properties and antimicrobial activity of azomethine monomer and oligomer based on 4-hydroxybenzaldehyde and 2-aminopyridine, Polimery 52 (2007) 827–835.
[10] I. Kaya, A. Bilici, M. Saçak, Synthesis, characterization and antimicrobial properties of oligo-4-[pyridine-3-yl-methylene) amino]phenol, J. Appl. Polym. Sci. 102 (2006) 3327–3333.
[11] M. Karakaplan, C. Demetgul, S. Serin, Synthesis and thermal properties of a novel Schiff base oligomer with a double azomethine group and its Co(II) and Mn(II) complexes, J. Macromol. Sci. Pure 45 (2008) 406–414.
[12] I. Kaya, M. Yıldırım, Synthesis and characterization of novel polyphenol species derived from bis(4-aminophenyl)ether: substituent effects on thermal behavior, electrical conductivity, solubility, and optical band gap, J. Appl. Polym. Sci. 110 (2008) 539–549.

[13] E. Tsuchida, H. Nishide, T. Nishiyama, The Cu-catalyzed oxidative polymerization of phenols, Makromol. Chem. 176 (1975) 1349–1358.
[14] T. Tema, S. Habaue, Highly selective oxidative cross-coupling polymerization with copper(I)-bisoxazoline catalysts, J. Polym. Sci. Part A: Polym. Chem. 43 (2005) 6287–6294.
[15] R. Cervini, X.C. Li, G.W.C. Spencer, A.B. Holmes, S.C. Moratti, R.H. Friend, Electrochemical and optical studies of PPV derivatives and poly(aromatic oxadiazoles), Synth. Met. 84 (1997) 359–360.
[16] T. Oguchi, S. Tawaki, H. Uyama, S. Kobayashi, Soluble polyphenol, Macromol. Rapid Commun. 20 (1999) 401–403.
[17] Y. Peng, H. Liu, X. Zhang, Y. Li, S. Liu, CNT templated regioselective enzymatic polymerization of phenol in water and modification of surface of MWNT thereby, J. Polym. Sci. Part A: Polym. Chem. 47 (2009) 1627–1635.
[18] A. Bilici, I. Kaya, M. Sacak, Oxidative polymerization of N_2O_2 type schiff base monomer and its metal complexes: synthesis and thermal, optical and electrochemical properties, J. Inorg. Organomet. Polym. 20 (2010) 124–133.
[19] F. Bruno, R. Nagarajan, P. Stenhouse, K. Yang, J. Kumar, S.K. Tripathy, L.A. Samuelson, Polymerizatıon of water-soluble conductive polyphenol using horseradish peroxidase, J. Macromol. Sci. Pure A38 (2001) 1417–1426.
[20] X.G. Li, J. Li, M.R. Huang, Facile optimal synthesis of inherently electroconductive polythiophene nanoparticles, Chem. Eur. J. 15 (2009) 6446–6455.
[21] K. Colladet, M. Nicolas, L. Goris, L. Lutsen, D. Vanderzande, Low-band gap polymers for photovoltaic applications, Thin Solid Films 451 (2004) 7–11.
[22] R.S. Premachandran, S. Banerjee, X.-K. Wu, V.T. John, G.L. Mcpherson, J. Akkara, M. Ayyagari, D. Kaplan, Macromolecules 29 (1996) 6452–6460.
[23] I. Kaya, F. Dogan, A. Bilici, Schiff base-substituted polyphenol: synthesis, characterisation and non-isothermal degradation kinetics, Polym. Int. 58 (2009) 570–578.
[24] I. Kaya, M. Yıldırım, Synthesis, characterization, thermal stability and electrochemical properties of poly-4-[(2-methylphenyl)iminomethyl]phenol, Eur. Polym. J. 43 (2007) 127–138.
[25] S. Dubey, D. Singh, R.A. Misra, Enzymatic synthesis and various properties of poly(catechol), Enzyme Microbiol. Technol. 23 (1998) 432–437.
[26] F.R. Diaz, J. Moreno, L.H. Tagle, G.A. East, D. Radic, Synthesis, characterization and electrical properties of polyimines derived from selenophene, Synth. Met. 100 (1999) 187–1931.
[27] V. Sinigersky, G. Kossmehl, L. Mladenovad, I. Schopov, Doped non-conjugated polymers with enhanced electrical conductivity, Macromol. Chem. Phys. 197 (1996) 1713–1720.
[28] J. Flynn, L. Wall, A quick, direct method for the determination of activation energy from thermogravimetric data, J. Polym. Sci. Part B: Polym. Lett. 4 (1966) 323–328.
[29] T. Ozawa, A new method of analysing thermogravimetric data, Bull. Chem. Soc. Jpn. 38 (1965) 1881–1886.
[30] W. Tang, Y. Liu, X. Yang, C. Wang, Kinetic Studies of the calcination of ammonium metavanadate by thermal methods, Ind. Eng. Chem. Res. 43 (9) (2004) 2054–2059.
[31] H.F. Kissinger, Reaction kinetics in different thermal analysis, Anal. Chem. 29 (1957) 1702–1706.
[32] T. Akahira, T. Sunose, Research Report of Chiba Institute Technology, no. 16 (1971) 22.
[33] H.L. Friedman, Kinetics of thermal degradation of char-forming plastics from thermogravimetry. Application to a phenolic plastic, J. Polym. Sci. C 6 (1965) 183–195.
[34] J.M. Criado, P.E. Sanchez-Jimenez, L.A. Perez-Maqueda, Critical study of the isoconversional methods of kinetic analysis, J. Therm. Anal. Calorim. 92 (2008) 199–203.
[35] S. Vyazovkin, Modification of the integral isoconversional method to account for variation in the activation energy, J. Comput. Chem. 22 (2001) 178–183.
[36] T. Wanjun, L. Yuwen, Z. Hen, W. Zhiyong, W. Cunxin, New temperature integral approximate formula for non-isothermal kinetic analysis, J. Therm. Anal. Calorim. 74 (1) (2003) 309–315.
[37] J. Criado, J. Malek, A. Ortega, Applicability of the master plots in kinetic analysis of non-isothermal data, Thermochim. Acta 147 (1989) 377–385.
[38] F.J. Gotor, J.M. Criado, J. Malek, N. Koga, Kinetic analysis of solid-state reactions: the universality of master plots for analyzing isothermal and nonisothermal experiments, J. Phys. Chem. A 104 (2000) 10777–10782.
[39] L.A. Perez-Maqueda, J.M. Criado, F.J. Gotor, J. Malek, Advantages of combined kinetic analysis of experimental data obtained under any heating profile, J. Phys. Chem. A 106 (2002) 2862–2868.
[40] F. Doğan, H. Akat, M. Balcan, İ. Kaya, M. Yürekli, Synthesis, characterization and thermal degradation kinetics of Poly (decametyhlene 2-oxoglutarate), J. Appl. Polym. Sci. 108 (2008) 2328–2336.
[41] K. Şirin, F. Doğan, M. Balcan, İ. Kaya, Effect of $CaCO_3$ filler component on solid state decomposition kinetic of PP/LDPE/$CaCO_3$ composites, J. Macromol. Sci. Pure 46 (2009) 949–958.
[42] F. Doğan, K. Şirin, İ. Kaya, M. Balcan, The influence of $CaCO_3$ filler component on thermal decomposition process of PP/LDPE/DAP ternary blend, Polym. Adv. Technol. 21 (2010) 512–519.
[43] J.H. Sharp, Sa. Wentwort, Kinetic analysis of thermogravimetric data, Anal. Chem. 41 (1969) 2060.
[44] W. Komatsu, Reactivity of solids, in: Proceedings of the 5th International Symposium, Elsevier, Amsterdam, 1965, p. 182.
[45] P.E. Sanchez-Jimenez, L.A. Perez-Maqueda, A. Perejon, J.M. Criado, Combined kinetic analysis of thermal degradation of polymeric materials under any thermal pathway, Polym. Degrad. Stabil. 94 (2009) 2079–2085.
[46] P.E. Sanchez-Jimenez, L.A. Perez-Maqueda, A. Perejon, J.M. Criado, Generalized kinetic master plots for the thermal degradation of polymers following a random scission mechanism, J. Phys. Chem. A 114 (2010) 7868–7876.